Politecnico Di Torino

Corso di Laurea Magistrale in Ingegneria Biomedica

Tesi di Laurea Magistrale

Detection of locomotion related events by electromyography analysis in non-human primates model of Parkinsons disease during gait

Supervisors

Prof. Marco Knaflitz

Ing. Flavio Rascellá

Candidate

Morena Raiola

S228297

A.A. 2017/2018

Contents

List of Figures

Abstract

The gait dysfunction in the Parkinson's disease(PD) could be improved through the spinal cord spatio-temporal stimulation at the lumbar level[5].
The spatio-temporal pattern of stimulation, coincident to motoneurons activation during gait cycle, could be provided by the detection of motor states related to lower-limb locomotion.
Here, the thesis project presents a comparative study on the discriminant analysis rLDA, QDA and RDA for the detection of locomotion related flexor-extensor events by electromyography (EMG) signal. Intramuscolar EMG signals, recorded from the lower-limb of a non-humane primates first in healthy condition and then affected by PD, are processed to built the detection.
The detection performance of three decoders are compared in terms of normalized mutual information in different tasks: (i) intra-day stability, to analyze the short-term behavior of EMG signal decoder by identifying gait events at different stages of PD; (ii) inter-days stability, to evaluate the longer-term behavior of the decoders by testing the performance over PD progression; (iii) stability over time, to estimate the decoders capability to preserve a constant trend the locomotion related events.
The resulting comparison returned rLDA as best candidate to detect the motor intentions in reasonable computational time. Moreover, the offline results have been backed up by the online simulation of rLDA for the real-time motor states detection.

Introduction

In the last two decades, several studies were focused on the alleviation of locomotion deficits using neuromodulation in animals with Parkinsons disease (PD) and spinal cord injury (SCI)[6–11]. PD and SCI cause an alteration or a rupture of communication pathway between the supraspinal and spinal neural network resulting in gait disorders. Therefore, the common aim of these researches is to restore the gait cycle creating an alternative communication way that translates the locomotor intention into muscular activation.

Different therapeutic approaches on humans have been performed[10, 12–14] but the benefits observed for the axial symptoms are limited. However, Capogrosso et al.[5] have shown a substantial system that may overcome the issues of the other studies. This study proposes a method to restore gait on non-human primates with spinal cord injury by brain-spine interface. Signal recorded from the motor cortex was used to train a decoder to predict the animal locomotor intentions. The decoded information was therefore used to modulate the neural afferent information involved during gait by spinal cord stimulation(SCS).

In this scenario, the presented master project is focused on the detection of locomotion events from electromyography signal of non-human primate affected by PD.

The detection of gait events by Machine Learning techniques, could represent a valid means able to predict the locomotor intentions of the animal. An exact classification of different gait phases could be essential to anable the indications for carrying out the spatio-temporal neuromodulation and improve the motor control in Parkinsonians.

In rehabilitation framework, therefore, the proposed detecting method could be an alternative solution to the invasive motor cortex decoder. Moreover, EMG based decoder could be also the key to bypass the influence of the alteration of motor cortex plasticity in PD[15] over the recorded signals.

Chapter 1

Parkinson's Disease

Parkinson's disease (PD) is a neurodegenerative disorder that effects more than ten million people all over the world[16]. It is the most common extrapyramidal[1] brain disease, characterized by a chronic and progressive clinical course.
The PD pathological characteristic is the continuous death of neurons in the *substantia nigra pars compacta*, located in the antero-superior part of the mid-brain, figure(1.1).

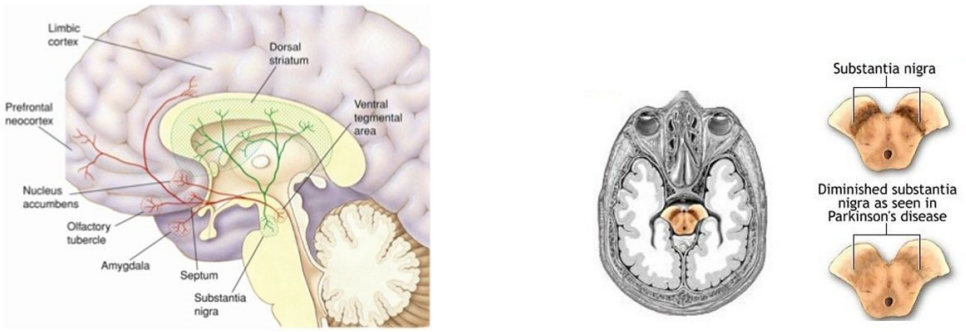

Figure 1.1: Simplified scheme of the neural structure in the *basal ganglia* involved in PD(on the left).Comparison between the *substantia nigra* in a healthy and PD affected individual(on the right)[1].

[1]The extrapyramidal system is a part of the motor system and it is responsible of body coordination. Its operating depends on dopamine neurotransmitter[17].

Dopaminergic neurons in the substantia nigra are the main source of neurotransmitter dopamine, that is responsible for relaying messages that control and plan body movements. The dopaminergic neurons death determinates an important dopamine deficiency, affecting the balance between direct, indirect, and hyper direct pathways among parts of brain. This altered communication influences the control of muscles and therefore locomotion.

1.1 Etiology

The exact cause of these neurons' death is still unknown, but many epidemiology studies[18, 19] have shown that a combination of genetic and environmental factors could be the cause. Unfortunately, how these two causes interact varies from person to person.

Regarding genetic factors, the directly disease inheriting is rare, in fact, only about 10 -15 % of all cases are thought to family history (monogenetic) while the other 85-90 % of cases are classified as sporadic (or occasional)[20]. Nevertheless, it is important to point out that even if a genetic mutation is present, increasing the risk of developing Parkinson, the chances of this happening are very low.

Conserning environment factors, they are connected especially to exposure to pesticides (e.g.Paraquat)[21], heavy metals (e.g iron, zinc, copper)[22] and hydrocarbon-solvents (e.g trichlorethylene)[23] used in industrial processes. However, a direct link between the exposure to the environmental factors and the development of the disease is still unclear.

1.2 Symptomatology

The disease affects all ethnic groups and both sexes, even if there is a small superior percentage in male sex[24]. The average age in which PD is more frequent is around 60 years, but about 5% of patients may present a premature onset between 21 and 40 years[25]. The effects are different from patient to patient and the symptoms can change from day to day.

The most common PD symptoms are:

- Resting tremor: most of the patients have a tremor and involuntary rhythmical movement, when they are at rest. It is usually a hand tremor, feet or jaw tremor, more evident on one side. It is caused by a rapid and repeated contraction and relaxation of muscles. Tremor may be symptom of disease onset, and often does not evolve over the years;

- Muscle rigidity: it is an involuntary increase in muscle tone that often starts on one side of the body. It usually effects the limbs, the neck and the trunk;

- Bradykinesia, Akinesia and Hypokinesia: bradykinesia is a slowness in carrying out or a difficulty in initiating spontaneous movements. Bradykinesia could affect one limb, one side of the body, or the whole body. Akinesia is referred to a loss of movement, for example, rarer eye blinks or lack of facial expression. Hypokinesia means a reduced movement, such as soft voice or (hypophonia)a small handwriting (micrographia);

- Balance problems: it is a symptom that involves "the body axis", it is due to a reduction in the rectification reflexes. The subject is not able to spontaneously correct any imbalances, increasing fall risk.
  Balance disorders do not respond to dopaminergic therapy so, phys-

iokinesitherapy becomes an important practice for the control of the disorder[26–28];

- Gait disorder: it consists of a reduction in the arms movement, a fixed posture in flexion and a shorter step. The patient sometimes tends to drag his feet on the floor and to pick up the pace to avoid falling. In this pathological condition, called "festination", the walk becomes like a short run.
  Moreover, episodes of "freezing" may affect locomotion. This phenomenon may result in impossibility to start walking, to change the direction or when the patient must cross narrow passages (like a door or a corridor).

In addiction to physical disorders, cognitive disorders, such as loss of smell sense and vision problems or/and non-motor symptoms, such as tiredness, depression and pain, may appear.

1.3 Diagnosis

Nowadays various types of scans allow to examine the anatomy and functionality of the brain. Magnetic resonance imaging (MRI)[2] is a non-invasive imaging technique, which uses radio-frequency electromagnetic waves to visualize soft tissue such as brain. In PD context, MRI exam could allow to visualize, on axial imaging, a loss of the normal swallow tail in the substantia nigra, as shown in figure(1.2).
Other imaging techniques are Single-Photon Emission Computed Tomography($SPECT$)[29] and Positron Emission Tomography(PET)[30].These two techniques belong to the nuclear medicine functional imaging technique that is used for the evaluation of presynaptic dopaminergic deficits.
In recent years, the new functional tomography method $DaTSCAN$ is taking

off. It is a scintigraphy technique, which consists in the injection of a particular tracer, ioflupane, into the vein to acquire with *SPECT* devices brain scans.

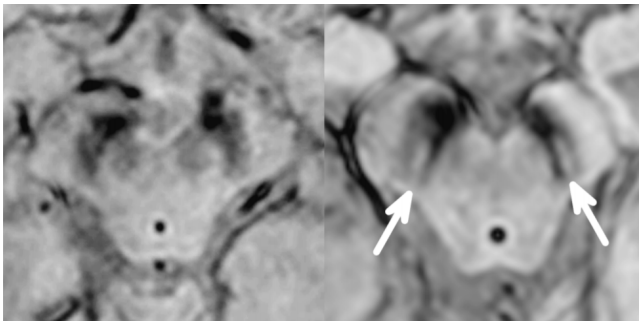

Figure 1.2: MRI images : substantia nigra of a PD patient (on the left) , substancia nigra of a non PD patient (on the right)[2].

DaTSCAN promotes the detection of nerve cells that release dopamine. This functional tomography can show a possible alteration of dopamine levels in the basal ganglia. The examination with *DaTSCAN* cannot be considered conclusive in the diagnosis of Parkinson, but undoubtedly a good neurological examination that can lead to a very accurate diagnosis[31].

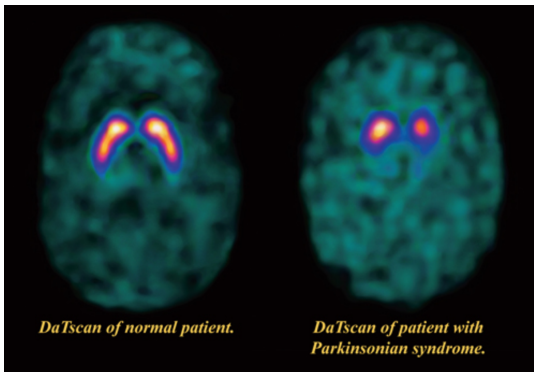

Figure 1.3: *DaTSCAN* of healthy subject on the left,*DaTSCAN* of Parkinsonian subject on the right[3].

1.3.1 Clinical evaluation

Different rating scales are used in Parkinson's[16], some of them are related to motor symptoms, such as Hoehn and Yahr Scale or Schwab and England Scale, other to non-motor symptoms, such as NMS Survey Scale.
Often, more than one scale is used to give a broader picture of symptoms. Thought Parkinsons rating scales it is possible to assess the symptoms of the condition. These rating scales provide information on the patient's quality of life.
Nowadays, the most used criteria is the MDS-UPDRS scale (Unified Parkinson's Disease Rating Scale, promoted by the Movement Disorder Society),a revision of UPDRS scale. In MDS-UPDRS scale, different elements of several scales, included non-motor symptom scales, are combined to produce a comprehensive tool to monitor the course of Parkinson's, in terms of the degree of disability.

According to the MDS-UPDRS[32] the evaluation state consists of four parts:
Part I: clinical evaluation about the mental state, on the basis of information about the behaviour and the mood given by patients;
Part II: self-assessment of daily activities (talking, swallowing, dressing, salivating, walking ...);
Part III: clinical evaluation of motor capacity;
Part IV: prognostic evaluation;

Any responses of MDS-UPDRS questionnaire is evaluated by a subscale divided in 5 values[32]: 0 = normal, 1 = slight, 2 = mild, 3 = moderate, and 4 = severe.

1.4 Therapy

At the moment there is no cure for Parkinson's, however medication can support the affected subjects reducing the effect of some symptoms . A wide range of medications is available.

The active substance at the base of most medication is the *levodopa*, which is made into dopamine in the body. Treatment with levodopa increases the quantity of dopamine in the body and so reduces PD's signs.

Other medications are mainly enzyme inhibitors, e.g. MAOB that block the dopamine destruction in the brain by particular enzymes[33].

In most current medicines, levodopa is associated with peripheral decarboxylases inhibitors[16]: *benserazide* allows more of the levodopa to get into your brain, before it is changed into dopamine; *carbidopa* is added to reduce the undesirable effects of levodopa (nausea, vomit, arrhythmias, mental disorders and dyskinesias).

However, the long-term efficacy of levodopa decreases, causing "dopa resistant" motor and "dopa resistant" non-motor symptoms; the first ones are linked to motor fluctuations, dyskinesias and freezing episodes, the second ones to mood and cognitive impairment[13].

To minimize such problems, in the last few years, different approaches are evaluated for the replacement of levodopa therapy.

Some researches begin to take into account the chronic electrical stimulation of subcortical brain structures as an additional treatment option for PD-patient. Initially, direct electrical stimulation of the subthalamic nucleus, also known as deep brain stimulation (DBS), seems to have some promising therapeutic effects. However it has shown its limits: DBS is an invasive procedure with a 4% risk of intracranial hemorrhage[34]. Moreover, its response is variable, the possibility of DBS surgery is limited to 14% of Parkinson patients[35], and DBS has not prolonged effects on axial motor signs(AMS)(speech, postural

instability and gait)[10].

In this context, a low-frequency stimulation of the pedunculopontine nuclei(PPN) has proposed to improve axial and postural symptoms, but results are still heterogeneous[14].

In the last 10 years, the researchers' attention is addressed to electrical stimulation of the spinal cord(SCS) to improve the postural instability and gait disturbance (PIGD)[36] and to have a better control of pain [37]. This alternative approach for symptomatic treatment of PD results less invasive than the other methods.

Chapter 2

State of the Art

Parkinson disease alters communications between supraspinal centres and spinal circuits responsible for lower limb locomotion, leading to gait disorders. However, neural networks on the spinal cord remain intact and able to reproduce a rhythmic activity if properly driven. Recently, spinal cord stimulation(SCS) has showed abilities to access surviving circuits and reduce locomotion deficits. This electrical stimulation strategy may be a solution to improve locomotion and axial symptoms in PD subjects, for which deep brain stimulation(DBS) and levodopa therapy alone are inconclusive[13, 14, 34, 35].

The first implementation of SCS for the treatment of movement disorders is described by Gildenberg in 1978[38]. Gildenberg used high-frequency dorsal column stimulator at the C1-C2 level to treat the spasmodic torticolli, but the discouraging results made his proposed therapy unpopular. However, after two decades SCS approach became the object of several studies [5, 9, 39]. The researchers showed how SCS could be used to alleviate motor disorders on animals with different pathologies.

One of the first study is led, in 2009, by Fuentes et al.[7]. Their analysis showed how, on Parkinsonian rats, high-frequency stimulation at the upper thoracic level can partially restore rats locomotion; in particular, this stimulation pro-

tocol reduced akinesia and bradykinesia problems.

Fuentes findings drove many researchers to deepen neuromodulation approach for alleviating motor symptoms of levodopa-resistant PD gait disorders.

In 2014, Santana et al.[8] showed a stimulation at high thoracic level (T3-T4) on male marmosets. An important reduction of motor deficits in particular in freezing, hypokinesia, and bradykinesia is observed. Nevertheless, during these studies, researches applied a continuous stimulation, under the assumption of an increase of the excitatory level of the neural network, regardless of the on-going movement.

Two years later, Wenger et al.[6], introduced the spatiotemporal neuromodulation therapy to improve the lower-limb motor control in rats after spinal cord injury(SCI). The new spatiotemporal SCS protocol considers that the hindlimb movements imply the activation of spatially motoneurons following precise temporal sequences, that are modulated through the proprioceptive feedback circuits. According to this hypothesis, electrical neuromodulation of lumbar segments has to reproduce specific spatiotemporal patterns of motoneuron activation identified by the respective extensor or flexor hot spots.

These new stimulation concepts improve gait quality, in terms of endurance and locomotion, and weight-bearing capacity, in several rodents affect by SCI.

Recently, Capogrosso et al.[5] used spatiotemporal SCS to restore lower-limb voluntary control on non-human primates with SCI.

The aim was to re-establish the lost communication between the brain and the spinal circuits, taking into account the motor intention of the animal to synchronize the SCS. This brain-spine interface is developed decoding the flexor-extensor motor states from leg motor cortex activity to trigger SCS. The brain controlled stimulation results to be efficient, in terms of the quantity and quality of foot steps.

Chapter 3

Materials and Methods

The following chapter describes the different steps for the building and the validation of the decoder, starting from the dataset construction.
Firstly, the target events are achieved by tracking from the video the frames corresponding to the start and the end of the gait stance phase[2]. Then, the EMG data collection is obtained through the elaboration of the EMG recordings.
Hence, the whole dataset is split in Training set, to build and validate the decoder and in Test set, to examine the decoder efficiency first offline and then online.
The last section describes the figures of merit used to estimate the decoder performance and the evaluation method of the events detection.

[2]The gait cycle is characterized by two different phases:(i)Stance phase, during which the foot is in contact with the ground;(ii)Swig phase, in which the foot is not in contact with the ground[40].

3.1 Data acquisition

3.1.1 Subjects

During the gait cycle analysis, one male rhesus monkey (Macaca Mulatta) are taken into account (M1).
The monkey, starting from a healthy condition, receive a gradually administration of 1-methyl-4-phenyl- 1,2,3,6-tetrahydropyridine (MPTP), a neurotoxin that targets specifically dopaminergic neurons that are involved in Parkinsons disease. Progression of the PD is daily assessed based on a mobility scale, also keeping track of the body weight of the animal (tab.3.1).

Days	**rif**	**MPTP injection**(mg/Kg)	**Weights**(Kg)	**PD Score**
23-11-2013	baseline	No	6.7	0
24-11-2013	baseline	No	6.7	0
09-01-2014	P25	1.38	6.9	2
16-01-2014	P32	1.36	6.8	2
30-01-2014	P46	1.32	6.6	6
06-02-2014	P53	1.32	6.6	6
21-04-2014	P129	STOP	6.6	6
23-04-2014	P131	STOP	6.6	6

Table 3.1: Control parameters of monkey M1.

3.1.2 Experimental Set-Up

The data recordings, acquired from monkey walking on a treadmill, are collected in order to develop the gait events decoder. Two kind of data are recorded: intramuscular EMG signals for muscles activity recording and video signal to keep track of the monkey's kinematics.

The intramuscular EMG signals are recorded using eight bipolar electrodes implanted in flexor and extensor muscles of the right leg,fig(3.1). Each muscular signal is pre-amplified and sent to a recording station (BlackRock® Microsystems) with a sampling frequency of 2 kHz.

Monkey locomotion is recorded by using SIMI®(Simi Reality Motion Systems, Germany) motion tracking system with a sampling frequency of 100 Hz.

During monkey training, the following muscles are recorded: gluteus medius (GLU), iliopsoas (IPS), rectus femoris (RF), semitendinosus (ST), gastrocnemius medialis (GM), tibialis anterior (TA), extensor digitorum longus (EDL), and flexor hal- lucis longus (FHL).

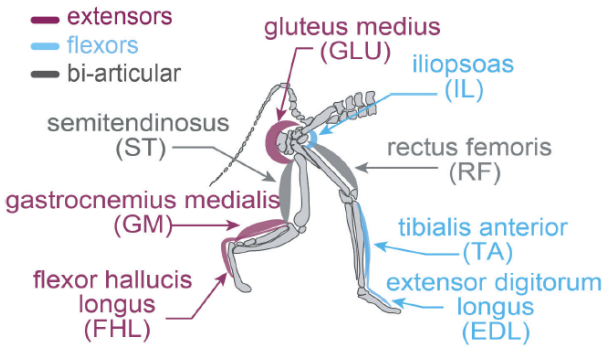

Figure 3.1: Hind-limb muscles in witch are implanted EMG electrodes [4].

3.2 Data construction

3.2.1 Target events construction

Before proceeding with the gait analysis, a recording archive has been created in which videos and correspondent EMG recordings are ordered by date.

The target events, useful to test the decoder, are extracted from the video in two different foot state: foot-off gait events(FO) and foot-strike gait events(FS).The defined targets are just related to the right leg only of the monkey.

By using MATLAB® software(Matlab R2016a, The Math Works inc.), target events collection is done pulling frames from the video matched with two-time instants: one, when monkeys foot gets off the ground (FO), the other when monkeys foot hits the ground (FS).
The frames range of not-gait cycle is tracked. In this way, the times when the monkey is climbing on the mirror or is involving in other activities, are marked.

3.2.2 Data pre-processing

The movement artifacts, mainly due to possible large movement of the monkey, are identified by setting a double threshold, as shown in figure (3.2), before processing the data.
In order to remove the noise, the samples exceeding the threshold values are not considered.

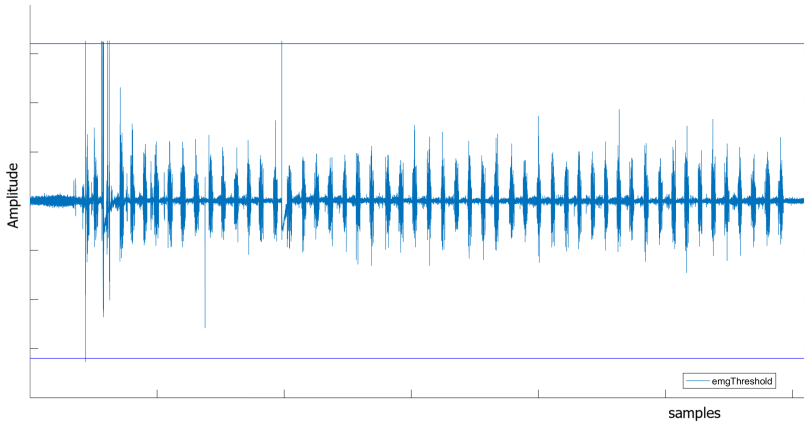

Figure 3.2: Raw EMG signal with threshold.For clarity, only one EMG channel is represented (channel 1).

On the other hand, the resulting raw EMG samples within the double-threshold identify "good-epoch" (GE) of different lengths, as shown in figure(3.3).

Moreover, periods in which the monkey has not a regular cycle gait are not considered in the analysis. Finally, in order to have useful raw data windows, among all GE, only those with more than 2000 samples and with at least one gait events(FS or FO) are considered.

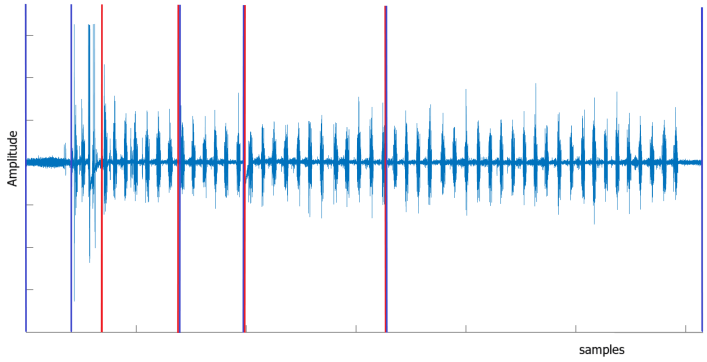

Figure 3.3: *Good Epochs* are bounded by two successive blue lines and two successive red lines. For clarity, only one EMG channel is represented (channel 1)

The considered GE are then processed according to the following steps fig(3.4) to obtain the EMG signal linear envelope:

1. To remove movement artifacts, the raw data are band-pass filtered in a frequency range 50-450 Hz by using a 4^{th} order (slope -80dB/dec) zero-phase Butterworth filter; this filter has the flattest band-pass zone. This filter has the flattest band-pass zone, that allows a low attenuation in the bandwidth.

2. To facilitate the interpretation, a linear envelope is implemented: first, the full-wave is rectified, then a 4^{th} order(slope-80dB/dec), zero-phase low-pass Butterworth filter with a cut-off frequency of 10 Hz is computed.

3. The linear envelope is finally normalized for each channel to uniform the different patterns.

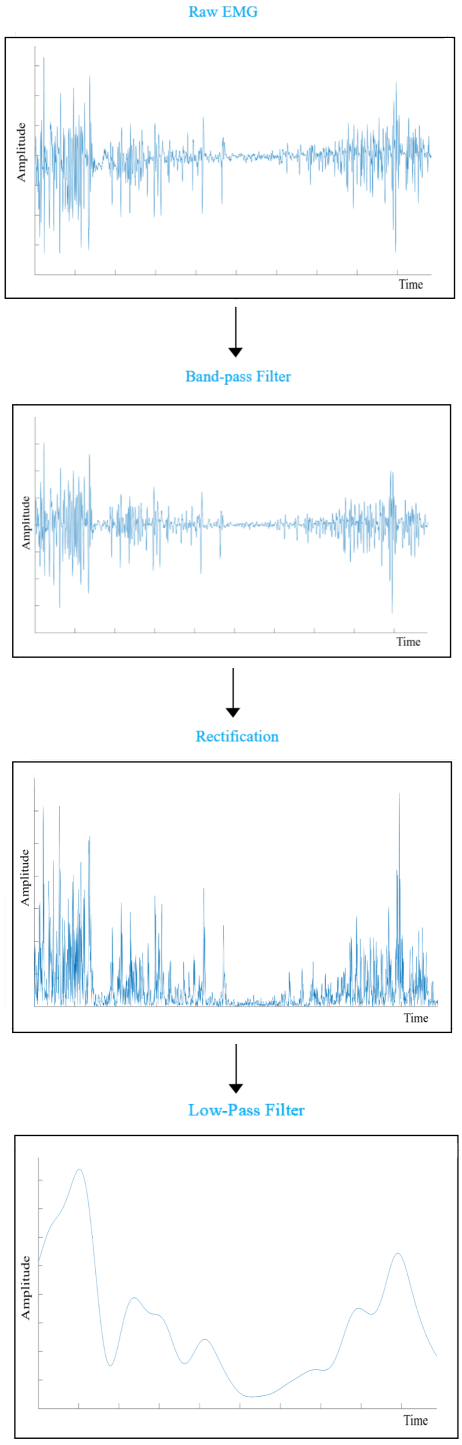

Figure 3.4: Pre-processing of raw EMG data to reduce movement artifacts: raw EMG data is filtered with a BP and rectified(pictures 1 to 3). In the forth graph, data is low-passed filtered and normalized between [0,1]. For clarity, only one EMG channel is represented (channel 1)

3.2.3 Data segmentation

The model selection is effectuated dividing the dataset into two parts: 70% Training set, 30% Test set. The Training data is used to build the initial detection model, while, the Test set is used to the final assessment of the model accuracy.

To make the model more general and less tied to the idiosyncrasies of Training set, the cross-validation is implemented. The Training set is split in two equal parts, each used first as a Training set and then as a Test set. Among the several models obtained with the cross-validation, the model resulting to have the highest performance is chosen as classifier. The classifier is then tested on the last 30% of the dataset to evaluate performance. The whole segmentation process is shown in fig.(3.6A), reported at the end of section 3.8.

3.2.4 Features extraction

The pre-processed data are elaborated as extract useful information to optimize the decoder implementation. Starting from the EMG processed signals a set of characterizing features are defined.

Training Set

Since, videos and EMG recordings have different sampling rates (100 Hz for videos, 2000 Hz for EMG signals), the FO and FS targets are synchronized. This step allows to trigger the time instant of the tracked events to the corresponding instant of muscular activation.

For each manual tracked event, FO and FS, a window (t_1,...,t_n) of a fixed number of previous samples is considered. In this window, the EMG amplitudes of five equidistant time points are extracted, fig.(3.6B), reported at the end of section 3.8.

The equidistant time points $t_1,\ldots,t_n$ are defined in this way :

1. t_1 is the time of the first feature associated with the FO/FS event;
2. n is the number of time points;
3. (t_n-t_1) is the length of the fixed window.

Therefore, computing the same extraction method on each EMG channel, the feature vector contains a number of $n_{time-points}$* $n_{channel}$ features for each FO/FS event.
The number of time points(n) and the length of the window(t_n-t_1) are two control parameters for the decoder. Even though these parameters are fixed at the beginning of the model building, they could change during the validation process as to improve the performance and to select the most performing model.

Test Set
As above, a sliding window is used on each GE testing data to extract relevant features from EMG signals. In this case, the upper boundary of the window matches the end of the GE, while the lower boundary corresponds to the sample following an interval equal in length to the fixed window ($t_1,\ldots,t_n$) defined for the Training set.
By shifting the window, the instances related to a number of equidistant time points $s_1,\ldots,s_n$ are individuated , where s_1 is the time corresponding to the last sample of the considered GE, n is the number of time points and s_n-s_1 is the temporal distance between the first and the last feature. The whole process is explained in detail in fig.(3.6C), reported at the end of section 3.8.

3.3 Decoder Building

The detection of gait cycle events is achieved by using Machine Learning techniques implemented on MATLAB software. In particular, a supervised learning technique is adopted, considering that the input features and the output labels are defined.

In this study, different discriminant models are implemented rLDA, QDA and RDA. These three classification models are based on the Bayes' rule, according to which events populations are known a priori and new observations are classified into one of the known populations based on the extracted features. Therefore, the event probability is based on prior knowledge of conditions related to the event, in this way:

$$Pr(G = k|X = x) = \frac{f_k(x)\pi_k}{\sum_{l=1}^{K} f_l(x)\pi_l}. \tag{3.1}$$

where:

- f_k(x) is the class-conditional density of X, the feature vector, in class G=k;
- π_k be the prior probability of class k, with $\sum_{k=1}^{K} \pi_k$ =1, where π_k=$\frac{\#ofSamplesInClassk}{\#OfSamples}$;

In discriminant analysis the class-conditional density follows a Gaussian distribution f_k(x):

$$f_k(x) = \frac{1}{2\pi^{\frac{p}{2}}|\sum_k|^{\frac{1}{2}}} e^{(-\frac{1}{2}(x-\mu_k)^T \sum_k^{-1}(x-\mu_k))}. \tag{3.2}$$

where p is the feature vector dimension, $\sum_k$ is the covariance matrix and μ_k is the class mean.

According to Bayes'rule, to obtain the decision boundaries δ_k(x), the (3.1) must be maximized. Hence for each considered model, δ_k(x) is achieved making

the product of the prior and the density of the Gaussian distribution f_k(x) maximum.

$$G(x) = arg_{max} Pr(G = k|X = x) \tag{3.3}$$

The discriminant analysis is chosen because the classification performance is similar to more complex classification algorithms such as MLP_NN and SVM. Moreover, LDA is also efficient in computational terms in real-time implementation[41, 42].

3.3.1 rLDA

Linear Discriminant Analysis (LDA)[43] is a linear classification method, so the decision boundaries δ_k(x) is a linear combination of features that best separates the classes.

In LDA, the classes have a common covariance matrix, so $\sum_k = \sum \forall k$.

The result of mathematical operations of (3.3), considering the homogeneous covariance matrices, defines the *linear discriminant functions* as:

$$\delta_k(x) = x^T \sum^{-1} \mu_k - \frac{1}{2}\mu_k^T \sum^{-1} \mu_k + log\pi_k. \tag{3.4}$$

where

$\mu_k = \sum_{g_i=k} \frac{x_i}{N_k}$ and $\sum = \sum_{k=1}^{K} \sum_{g_i=k} \frac{(x_i-\mu_k)(x_i-\mu_k)^T}{N-K}$;

In this study, for the detection of gait events, the implemented LDA model is based on *linear discriminant functions* in which the covariance matrix $\sum$ depends on a control parameter $\alpha \in$ [0,1]:

$$\sum(\alpha) = (1-\alpha)\sum + \alpha\sigma^2 I \tag{3.5}$$

Assuming that FO/FS class priors are equals, the prior probability, logπ_k, is neglected.

Moreover, since the covariance matrix $\sum$ defined in (3.4) is substituted by $\sum$ in (3.5), it is necessary to ensure that $\sum$ is not singular, to allow to make it invertible. For this reason, when the $\sum$ is singular the regular coefficient α is equal to Cholesky factor ($\alpha = 10^{-6}$).From this prospective, the implemented LDA takes the name of rLDA, where "r" means *regularized*.

3.3.2 QDA

Quadratic discriminant analysis(QDA)[43] is a classification problem, where the covariance matrix is not identical for each classes but it is different for every k. Hence, for QDA the decision boundary is determined by a quadratic function:

$$\delta_k(x) = -\frac{1}{2} log|\sum_k| - \frac{1}{2}(x-\mu_k)^T \sum_k^{-1} (x-\mu_k) + log\pi_k. \tag{3.6}$$

3.3.3 RDA

Regularized discriminant analysis(RDA)[43] is an intermediate between LDA and QDA, developed by J. Friedman. RDA shrinks the different class covariances of QDA toward the common covariance as in LDA, through two different control parameters α and γ, both $\in$ [0,1].

The regularized covariance matrices have the form :

$$\sum_k(\gamma) = (\gamma)\sum + (1-\gamma)\sum. \tag{3.7}$$

Replacing $\sum$ in (3.7) with $\sum$ (α) of (3.6), a general family of covariances $\sum$ (α, γ) is obtained.

So:

$$\sum_k(\alpha,\gamma) = (\gamma)\sum_k + (1-\gamma)(\sum(1-\alpha)\sum + \alpha\sigma^2 I). \tag{3.8}$$

In an extreme case, if $\alpha = 1$ and $\gamma = 1$, then the second term in (3.8) is zero and a QDA is obtained. If $\alpha = 0$ and $\gamma = 0$ an LDA is realized.

In summary, rLDA, QDA and RDA algorithms return classification rules to define the estimated the class to which gait events belong. Therefore, in order to achieve the classification rule the Gaussian distribution parameters need to be estimated from the Training data extracted earlier.
Once these parameters have been defined, the *linear discriminant function* δ_k can be determined. Hence, according to the discriminant functions, it's possible to choose for each Test sample a class. In particular, the detected event may be classified in the FO or FS class with a certain probability; otherwise the testing sample is predicted in the "non-event" class. In order to decide the estimated class, the event must exceed a minimum probability value of 85%. Furthermore, two or more estimated events of the same class FO/FS detected within a time interval of 500 ms are not considered. The latter choice is done to ensure a natural succession of gait steps.

3.4 Model Validation

In a second step, the decoder building, be it rLDA, QDA or RDA, is validated through cross-validation. The cross-validation technique is implemented to improve the performance model making it more general and less tied to the Trainig set. As already mentioned, whole EMG Dataset, built to implement the detection algorithm, is split into two groups: the Training set, used to build and validate the initial model, and the Test set, used to estimate the figures of merit of the model.
During the cross-validation, the Training data is used in this way: the original samples, belonging to Training set, are partitioned into two equal sized subsamples. In the first step, one subsample group is retained as the Test set to estimate the decoder performance, and the remaining group is used as Training data; in the second step, the subsample group are inverted.

In the cross-validation, control parameters have been changed to estimate the best classifier model. The validation is implemented for each classifiers (rLDA, QDA, RDA), therefore, depending on the type of classifier, the control parameters change.

1. rLDA

   To find the optimal model, in the linear discriminant analysis, the following parameters are changed:

   - t_n-t_1, the length of the window that slides along the Training set by varying the distance between the samples, of which the EMG amplitudes are defined as features. The window length can assume two different values : 500 ms(1000 samples), or 300 ms(600 sample);
   - n, the number of features taken in account can change from 5 to 3. In other words, the number of equidistant samples, of which the EMG amplitudes are defined as features, change;
   - α, the regularized coefficient can change between [0,1], so the rLDA can move toward LDA model, or QDA model, by changing its matrix covariance value.

2. QDA

   In the quadratic discriminant analysis any regularized coefficient is defined, considering that QDA, for its decision boundary, takes in account only the inter class covariance matrix, different for each class k.
   While the following parameters change:

   - t_n-t_1, the sliding window length changes in 300ms, or 500 ms;
   - n, the number of features, in the chosen window, can be 5 or 3;

3. RDA

   For RDA, more control parameters change, in fact, in addition to the

length of the window(t_n-t_1) and the number of equidistant points(n) to be considered as features, there are two variables coefficients of regularization:

- α and γ both $\in$ [0,1];

3.5 Figures of Merit

The accuracy of the decoder is described by measuring how well it performs in terms of mutual information C_{xy}, a metric incorporating both sensitivity and specificity of the detector[44].
The value of the C_{xy} is chosen to estimate the correlation between the times of real events and a the times of detected events, in this way:

$$I(X,Y) = \sum_X \sum_Y p(x,y) log_2 \frac{p(x,y)}{p(x)p(y)} \tag{3.9}$$

where X and Y contain respectively all possible states of the real and detected events, while x and y are specific states from X and Y; p(x,y) is the joint probability, p(x) and p(y) are the probabilities of specific states, p(x)= $\sum_k RealEvents$ and p(y)= $\sum_k DetectedEvents$.
The maximum value of the mutual information is obtained when detected event times correspond to real event times. In this case, the mutual information value, C_{XY}, is normalized:

$$C_{XY} = \frac{I(X,Y)}{H(X)} \tag{3.10}$$

where H(X) is the entropy of real event times:

$$H(X) = -\sum_X p(x) log_2(p(x)) \tag{3.11}$$

The C_{XY} value is chosen as the model selection criteria in the validation model.

3.6 Detection Accuracy

The detection probability of the FO and FS events is estimated considering a Δt temporal tolerance. The Δt represents the time gap that could occur between the instant times of an estimated event and the instant times of a real event. Any detection within the tolerance window Δt is counted as a true positive detection. The time samples, not identified as FO/FS events, are defined as "non-event", in fig(3.5).

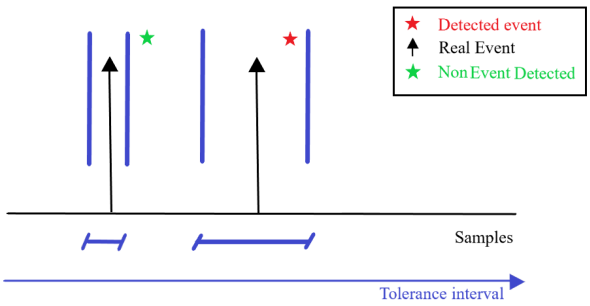

Figure 3.5: The detection probability of events is related to the rising tolerance intervals. Estimated events out of the tolerance interval is considered as not-event detected(green star); detected event within the tolerance interval is estimated as detected event(red star).

Since, the decoder is able to detect the event with a certain delay, it was useful to evaluate the performance, C_{XY}, according to the temporal accuracy of detection. For each model, 15 C_{XY} values are obtained corresponding to the same number of tolerance values ranging from 25 to 200 ms.

3.7 Statistical Analysis

On first assessment, the decoder performance is estimated in terms of the C_{xy} value at various tolerance interval. The estimation of the values are reported as mean and 95% confidence interval (CI).

To define the CI and obtain the C_{xy} mean value, the dataset is firstly parti-

tioned in N sessions. Afterwards, the decoder is trained on N-1/N sessions, and tested on the remaining one. This process is repeated for all N sessions. In this way a population of N values of C_{XY} is obtained for each implemented decoder methods.

For estimating the mean with 95%CI, a t-interval is considered, since the considered population is small and their variance is unknown.

The formula for a t-interval is:

$$\bar{x} \pm t_{(n-1;\frac{\alpha}{2})} \frac{\alpha}{\sqrt{n}} \tag{3.12}$$

where $t_{(n-1;\frac{\alpha}{2})}$ is a critical value of t-distribution, α is the population standard deviation and n is the number of values belonging to the considered population. The $t_{(n-1;\frac{\alpha}{2})}$ value depends on the number of values(n) through the use of "degrees of freedom" defined as df=n-1. Its value is looked up on a table.

3.8 Online Model

In order to dynamically test the decoder, an online model is implemented. It is generally known that the online performances of decoder are worse than its offline performances. Hence, online testing can be considered as a practical way of to identify the performance of decoders.

The real-time simulation is implemented on rLDA model because of its efficient in computational terms[42].

According to online model, EMG data is available in a sequential order and are tested at each step and not on the entire recording. The decoder operates periodically at 10 ms intervals, when Black Rock system provides the data. EMG test data is rescaled in [0,1] range, according EMG training data.

In this case, the features extraction (see fig.(3.6C)) is realized taking into account a period of 500 ms, stored into a buffer, prior to the event to be classified.

Moreover, the class of the detected event is decided by setting a threshold equal to 85%. Then, to ensure the physiological time of the gait steps, the detected consecutive events of the same class a 500 ms apart are not considered.

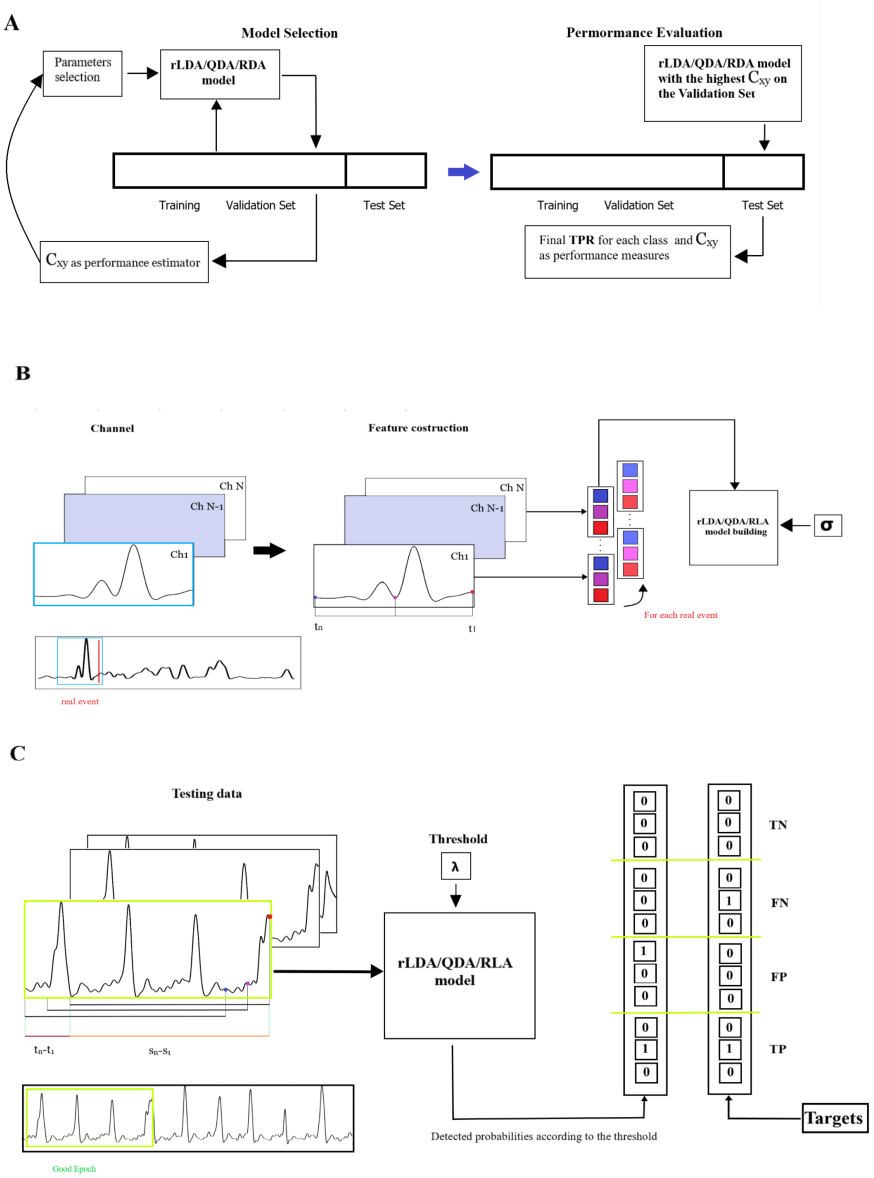

Figure 3.6: Flow of the detection algorithm.

A) Method used to partition the dataset into two independent sets: 70%Training set to built and validate the model, 30% Test set to estimate the model accuracy. B)Features extraction in Training set. For each target event a window of a fixed number(t_n-t_1) of samples is individuated(blue window). EMG amplitudes corresponding to n equidistant points(red,violet,blue) are taken as

features. The same number of features are considered for each channel and use for decoder building(rLDA/QDA/RDA).

A control parameters set σ are considered in order to take into account the decoders characteristic coefficients. C) Features extraction in Test set. In each GE (green window), a number of points equal to n is marked. The points (red, blu, purple) are individuated by a sliding window S_n-S_1 along the GE. Hence, the EMG amplitudes related to these marked points are considered as features. The rLDA/QDA/RDA algorithm implementation returns for each sample a probability values of belonging to each of the three classes(FO/FS/non-event). To decide the estimated class, the event must exceed a threshold λ. On the right the performance evaluation rule is described as a binar combination related to tolerance interval.

Chapter 4

Results and Discussions

In the following chapter, the performance for rLDA/QDA/RDA decoders are illustrated.

The first assessment is carried out on the recordings of healthy monkey M_1, comparing the offline decoders performance in terms of the normalized mutual information C_{XY} at different tolerance interval.

At a later stage, the decoders stability over Parkinson disease progression is evaluated: firstly, evaluating the *intra-day* decoders performance and then the *inter-days* decoders performance. The *intra-day* performance allows to evaluate the decoder model efficiency corresponding to different PD score. Indeed, the decoder is trained and tested on dataset belonging to the same day and by evaluating its performance at one PD score. On the other hand, *inter-days* performance are achieved by training and testing the decoders on different dataset. This modus operandi enables to evaluate the built decoders over the PD progression by analyzing the long-term behaviour of the EMG decoders.

Furthermore, it was considered appropriate to estimate the stability of the decoders over time.

The last aim is to evaluate the offline decoder performance by implementing

an on-line simulation.

4.1 Decoder Performance

4.1.1 Offline decoder performance

The evaluation criteria used to compare the gait decoder is the normalized mutual information C_{XY}, a metric that incorporates both sensitivity and specificity.

In the figure(4.1) below, the trend of the mean values C_{XY} for different tolerance levels, using a confidence interval fixed at 95%, is illustrated. Overall

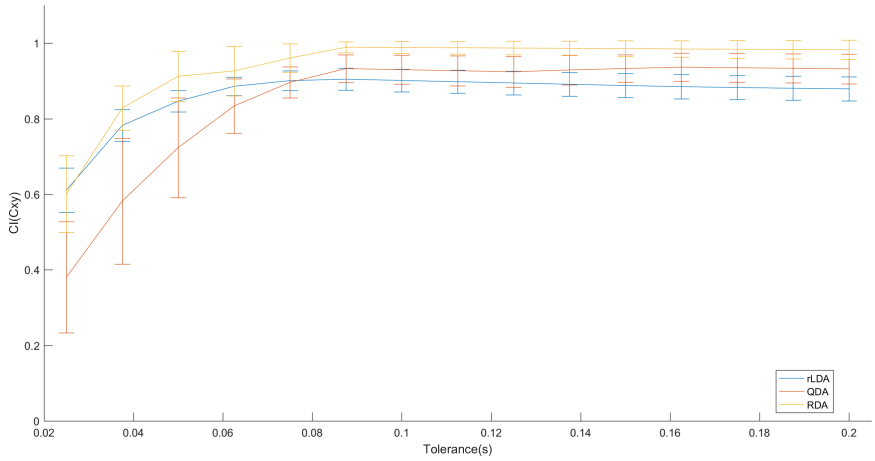

Figure 4.1: C_{xy} comparison among rLDA, QDA, RDA for different values of tolerance. Each result is reported as mean and 95%CI(vertical lines)

rLDA, QDA and RDA show the worst performances for tolerance ranges less than 75 ms. Moreover, the C_{XY} values estimated for these tolerance intervals values are characterized by a great variance compared to the values of C_{XY} obtained for higher tolerances ranges, fig(4.2).

It is evident that results related to QDA for lower tolerance ranges reflect a large discrepancy between the values obtained in the CI evaluation. On the

other hand, the statistic analysis in rLDA and RDA confirms that survey results are reliable.

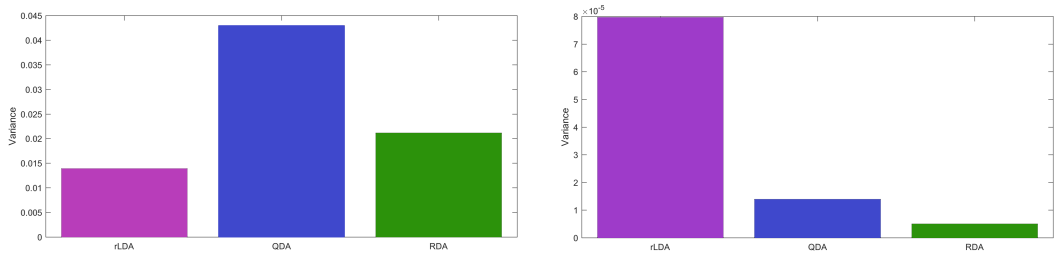

Figure 4.2: Variance of mean C_{xy} values in rLDA, QDA and RDA for tolerance ranges below 75 ms(on the left). Variance values of each decoders in correspondence of tolerance intervals larger than 75 ms(on the right).

It is clear that, rLDA, QDA and RDA decoders return higher value of C_{XY} in correspondence to greater tolerance. However, it is inconvenient to detect event using wider tolerance range since it would mean a lost of time resolution. Therefore, a tolerance interval limit equal to 200ms has been chosen, that represents a value corresponding to about one-quarter gait cycle of the healthy monkey.

In order to have a complete perspective on the performance, the mean computation time for decoders building is evaluated. In particular, the computational times are related to the validation phase, in which the rLDA models are constructed by chancing four control parameters, those of the QDA are defined by replacing two control parameters and finally the RDA models are built by varying five parameters of control (Materials and Methods section 3.4). It is clear that the RDA decoder takes longer computation times, as the number of built models are increased by one factor. In the context of brain-spine interface, the decoder could be used to modulate the information involved during gait and trigger the spinal cord stimulation. Hence, in the evaluation of the decoder performance, from here on out, a tolerance interval has been chosen equal to

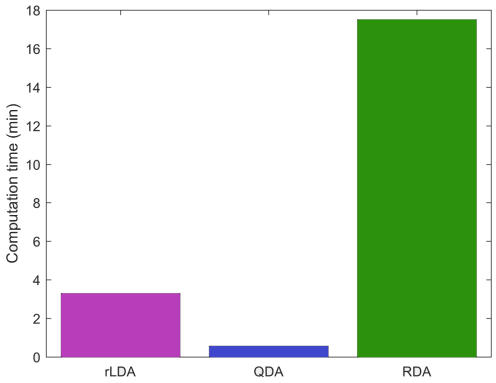

Figure 4.3: Mean values of computational time in rLDA, QDA and RDA related to the offline decoder models built in fig.(4.1).

75ms; this could be a good compromise, between the desired performances and the temporal accuracy in the detection.

4.1.2 Online decoder performance

The implementation of the online model can be considered as a further test to quantify the decoder performance.
The results are implemented only for rLDA decoder, which has shown good attitudes in the offline model[42].
The performance of the online decoder is compared with those obtained from the implementation of the offline decoder. The first assessment is realized comparing the figure of merit(C_{xy}) chosen for the statistical analysis. Figure(4.4) shows a decrease equal to 30.7% of performance in online model comparing to offline implementation.

Moreover,the comparison is made on the FO and FS classes, comparing the mean values of true positive rate(TPR)[3] on five detector models, each one built

[3]True Positive Rate (TPR) is defined as the number of true positive detections (N_{TP}) divided by the number of real events equal to the sum of true positive detections and false negative detections (N_{FN})

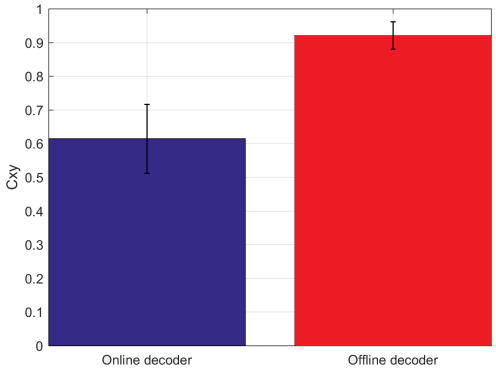

Figure 4.4: Performance statistical measures of C_{xy} in online model (on the left) and in offline model (on the right).

and tested on datasets of the same day. Two dataset related to the healthy monkey and three in which the monkey has different PD score values are chosen as to test the performance of the classifier during PD progression. The variability of the resulting TPR is taken into account by using the standard deviation parameter.

The results achieved show that the performance of the online decoder is lower than those of the offline classifier. In detail in fig(4.5), the decrease in performance is about 25.8% for the TPR related to FS class and 7.6% for the FO class.

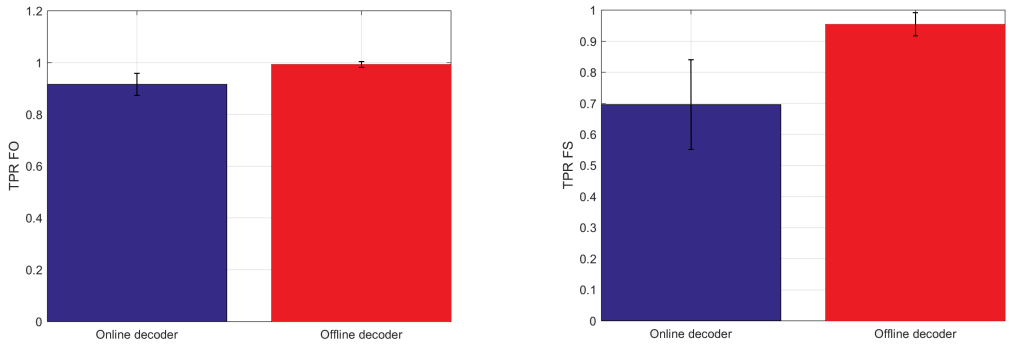

Figure 4.5: Performance statistical measures of TPR in online model and in offline model(FO on the left, FS on the right). Vertical lines report the standard deviation values.

4.2 Decoder Stability

4.2.1 Decoder Stability intra-day

In figure (4.7) below are set out the performance of rLDA/QDA/RDA decoders during the PD progress of M_1. To compare the decoders ability to detect gait events at different PD score, the evaluation criterion used is the C_{XY} value. In the graph (4.7), at each points correspond a C_{XY} values obtained by processing data recorded in the same day. In particular, eight intra-day dataset are taken into account to validate the decoders performance over PD progression ((4.6)): two related to M_1 in healthy condition, and six related to M_1 condition after MPTP injections (grey line). In addition, for each examined day, the rela-

Days	PD Score	MPTP injection
-23	0	no
-22	0	no
24	2	yes
31	2	yes
46	6	yes
52	6	yes
126	6	STOP
128	6	STOP

Figure 4.6: Summary table related to the injection of MPTP in M_1: temporal distance of the dataset taken into account from the beginning of the injections (grey line); PD score value; indications on the neurotoxin daily initiation.

tive PD Score of M_1 is reported. The results achieved show clearly that RDA (green line) decoder has detected the gait events at best. The C_{XY} values has not undergone significant fluctuations in 150 days interval corresponding to

PD. Hence, RDA has given a demonstration of good performance and adaptation in gait events detection in M_1 both in healthy conditions and in severe PD conditions. On the other side, QDA (blue line) decoder has not match

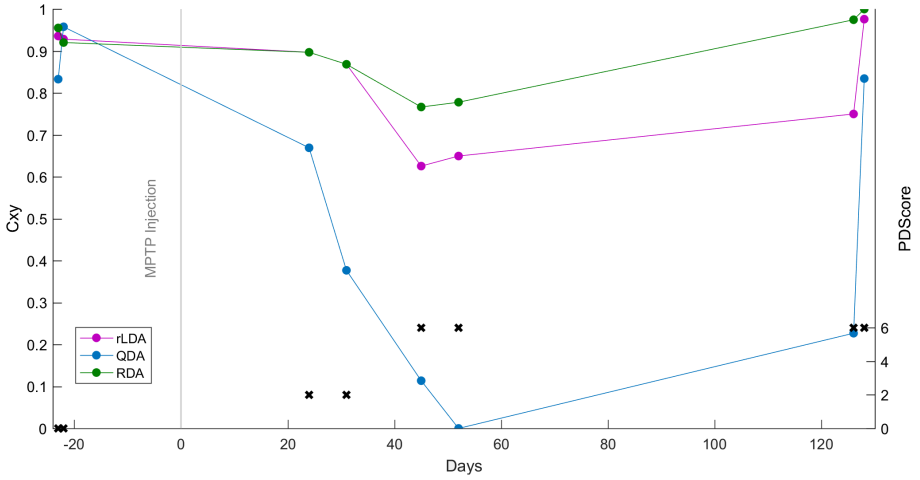

Figure 4.7: Decoder performance on intra-day data during PD progression. Pink line follows the rLDA evolution in 151 days interval, while blue and green lines are respectively related to development QDA and RDA over the disease in the same time interval. Grey line marks the beginning of MPTP injection. The black crosses indicate the monkey's PD score.

the expected trendline. The QDA shows its better performances mainly, in correspondence of the days before MPTP injection. Only in one case, during PD progression, QDA has shown good value of C_{XY}, but it is not statistically significant.

rLDA (pink line) performance has shown a trend similar to that of RDA within the first 35 days from the MPTP injection. Then, C_{XY} values are decreased holding good performance.

There appear to be an unstable C_{XY} region across the time between 40-50 days after neurotoxin injection, common to all decoders performance. This significant decrease may not be related to the monkey PD score. It could depend on the time gap between the time of injection and the time in which M_1 is trained. In this region where all the classifiers have shown the worst perfor-

mance, the monkey has a PD score of six after having received the injection MPTP. However, the decoder performances, 151 days after the first injection, have shown an increased even if the PD score of M_1 is remained constant. This result could be due to the fact that, in the last two days assessed, the injection of MPTP is stopped (see fig.(4.5)), thus the gait cycle of the monkey may no longer be influenced by the immediate effects of neurotoxin injection.

4.2.2 Decoder Stability inter-days

The graphs in fig(4.8) show the performances of rLDA/QDA/RDA decoders related to eight different intra-day dataset. The considered models follow the chronological progress of PD in M_1 (see fig.(4.5)). The aim of this assessment is to test the detection capacity of classifiers built on a fixed model during the whole window of observation of the course of the PD under consideration.
The graphs report on each row the C_{XY} values calibrated on one daily session and tested on other sessions. The C_{XY} values correspond to detecting tolerance of 75 ms. Thus, for each calibration session it is possible to evaluate the correspondent decoder attitude to detect the gait events in EMG signals recorded in different PD stages of M_1.

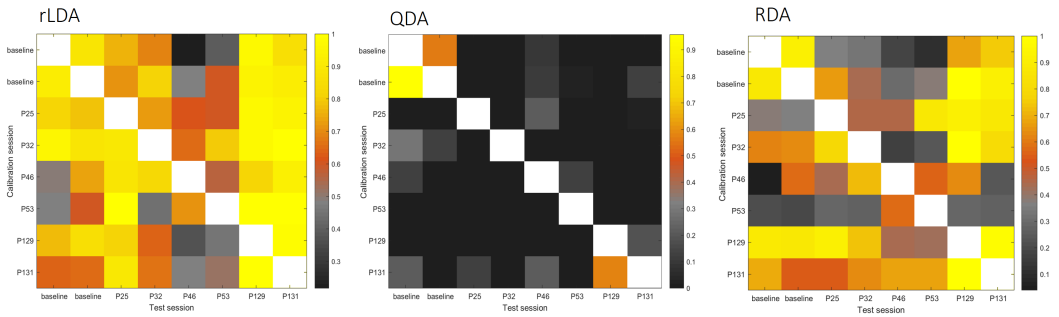

Figure 4.8: Decoder performance on inter-days data during PD progression.

Comparing the results obtained, it can be clearly seen that the rLDA classifier yields better performance than the QDA and RDA classifiers.

QDA decoder shows the worst longer-term behavior, no built model has proved its capability of detecting significantly gait events in monkey affected by PD. These results could be related to the specialization of the decision boundaries in QDA model on the Training set.

Both rLDA and RDA show significant results. The best achievements, by testing the decoder stability over PD, can be observed in correspondence of first two lines (baseline). Indeed the results, obtained by testing the baseline sessions relating to the healthy monkey, shown significant C_{XY} values, especially in rLDA. Here again, an unstable C_{XY} region (P47-P53) has appeared across corresponding to the time between 40-50 days. P47 and P53 sessions are referred to two injection days in which monkey shows PD score equal to six(see fig.(4.5)).

4.2.3 Decoder Stability over time

Moreover, the same C_{XY} values, used to validate the built model stability inter-days over PD, are fitted as shown in fig.(4.9). The C_{XY} values are plotted in function of the time distance between the session to calibrate the decoder and the session to validate it.

Therefore, it is possible to estimate the stability of the decoder over time. The rLDA chart demonstrates the decoder temporal robustness in 151 days interval, in which the decoder trend remain constant.

As achieved with the previous results, QDA shows the lowest performance in events detection. Moreover, the decoder ability to detect gait events decreases dramatically within few days.

The last result is related to the stability of RDA decoder, which does not show a relevant trend decrease.

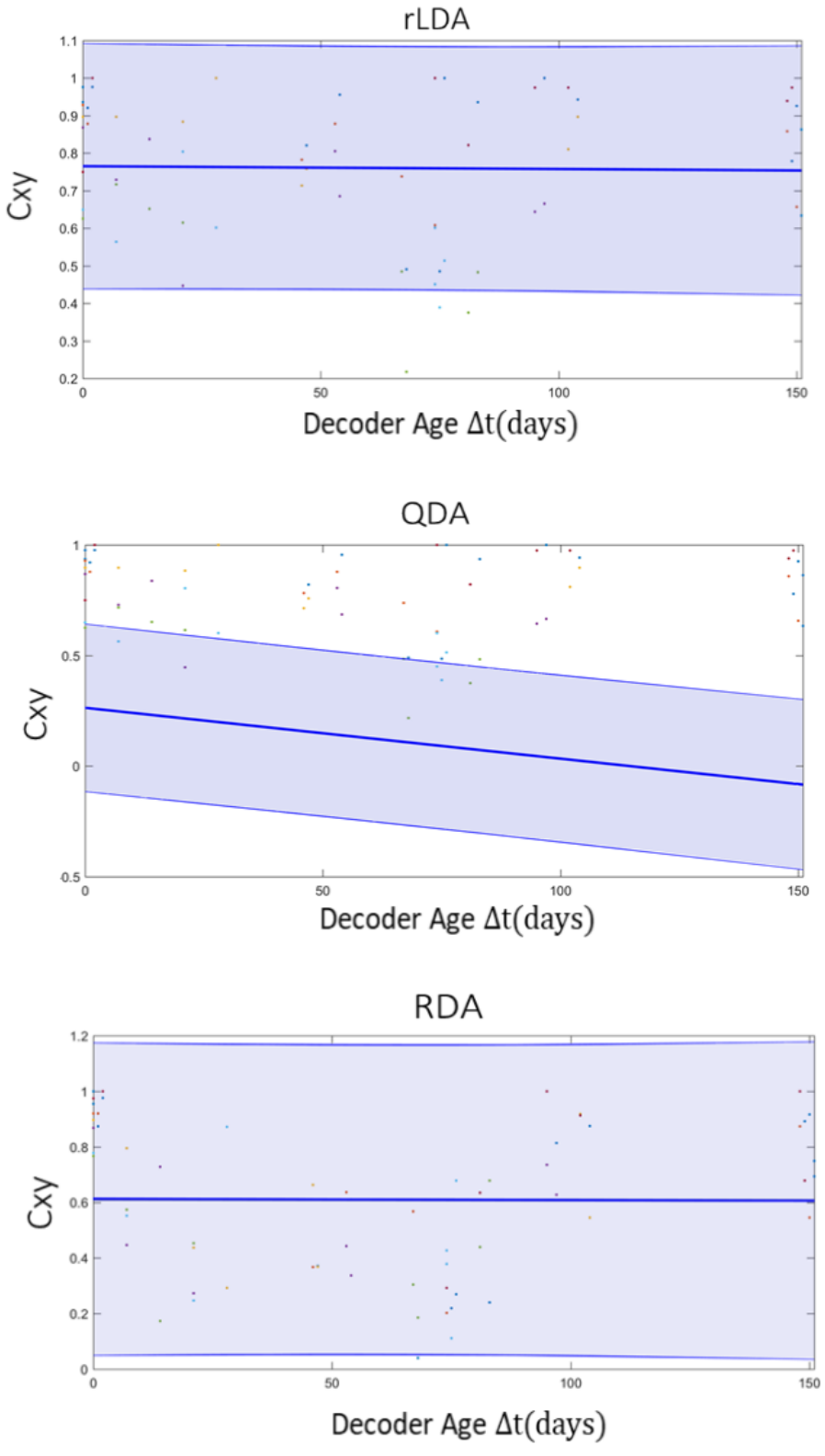

Figure 4.9: Stability over time of rLDA/QDA/RDA decoders represented as linear regression(blue line) and 95% confidence interval(blue rectangle)

Chapter 5

Conclusion

In this thesis has been implemented a decoder able to detect the flexor-extensor motor states starting from the EMG activity of a non-human primate's lower limb. The ultimate goal is to create an instrument able to detect the locomotion related events (FO and FS) as to support the subject by using an electrical spinal cord stimulation.

Machine learning discriminant analysis based techniques have been used. Indeed, three different classifiers have been implemented: rLDA, QDA and RDA. The initial set of measured EMG data is pre-processed in order to remove the movement artifacts and ensure a useful features extraction. The discriminant analysis based algorithms have been tested on the dataset, comparing their performances in terms of normalized mutual information (C_{XY}).

The resulting performances of the rLDA, QDA and RDA decoders indicate that QDA shows the worst performance both in the intra-day and in the inter-days models. Hence, the QDA based decoder is not able to track muscular patterns and identify gait events as well.

Overall, rLDA and RDA yielded essentially the same performance. rLDA has proved to be more flexible during the inter-days events detection testing mode. On the other hand, RDA has shown better performance in detecting events

during the intra-day testing models. Both decoders have shown constant trend over time.
Besides, RDA has the drawback that an higher number of control parameters need to be estimated during the validation phases, as to increase the computation time of the algorithm.
In first analysis, therefore, the rLDA is the best candidate for detecting locomotion events, the difference between the decoded and intended locomotion events is not noticeable both in intra-day and in inter-day testing.
A further test to estimate the rLDA performance is implemented by an on-line simulation. The online testing performance of the rLDA decoder has show good detection capabilities. The estimated C_{xy} value decrease, even if not negligible, allow a detection of true positive events over 70%.

The next step would be to evaluate the robustness of the decoders by testing the classifiers performances on more monkeys. In this way the results may be validated and may be asserted to be successful even when applied on different EMG recordings.
Since the ultimate goal of the decoder is to detect the events as to trigger the matching electrical spinal cord stimulation, it is needed to verify the decoder performance also combining the electrical stimulation at lumbar level. In fact, it is necessary to evaluate the influence of electrical stimulation on the EMG signal and on the events detection. In the first analysis, the stimulation should not have considerable effects on the detector, since the additive effect in amplitude of the stimulation is constant and is modulated during the pre-processing phase. In view of future applications, the evaluation of online decoder performance is necessary to ensure sufficient detection of the locomotion events and decrease the errors in movement decoding.

Bibliography

[1] URL `http://www.parkinsonassociation.org/`.

[2] Stefan T Schwarz, Mohammed Afzal, et al. The swallow tailappearance of the healthy nigrosome–a new accurate test of parkinson's disease: A case-control and retrospective cross-sectional mri study at 3t. *PLoS One*, 9(4):e93814, 2014.

[3] URL `https://www.cedars-sinai.edu/`.

[4] Marco Capogrosso, Tomislav Milekovic, et al. A brain–spine interface alleviating gait deficits after spinal cord injury in primates. *Nature*, 539 (7628):284, 2016.

[5] Marco Capogrosso, Tomislav Milekovic, et al. A brain–spine interface alleviating gait deficits after spinal cord injury in primates. *Nature*, 539 (7628):284, 2016.

[6] Nikolaus Wenger et al. Spatiotemporal neuromodulation therapies engaging muscle synergies improve motor control after spinal cord injury. *Nature medicine*, 22(2):138, 2016.

[7] Miguel Fuentes, Romulo Nicolelis et al. Spinal cord stimulation restores locomotion in animal models of parkinson's disease. *Science*, 323(5921): 1578–1582, 2009.

[8] Maxwell B Santana, Pär Halje, et al. Spinal cord stimulation alleviates motor deficits in a primate model of parkinson disease. *Neuron*, 84(4): 716–722, 2014.

[9] Grégoire Courtine et al. Transformation of nonfunctional spinal circuits into functional states after the loss of brain input. *Nature neuroscience*, 12(10):1333, 2009.

[10] Alfonso Fasano et al. Axial disability and deep brain stimulation in patients with parkinson disease. *Nature reviews Neurology*, 11(2):98, 2015.

[11] Monika Pötter-Nerger and Jens Volkmann. Deep brain stimulation for gait and postural symptoms in parkinson's disease. *Movement Disorders*, 28(11):1609–1615, 2013.

[12] Frances M Weaver, Kenneth Follett, et al. Bilateral deep brain stimulation vs best medical therapy for patients with advanced parkinson disease: a randomized controlled trial. *Jama*, 301(1):63–73, 2009.

[13] BR Thanvi and TCN Lo. Long term motor complications of levodopa: clinical features, mechanisms, and management strategies. *Postgraduate medical journal*, 80(946):452–458, 2004.

[14] Elena Moro, Clement Hamani, et al. Unilateral pedunculopontine stimulation improves falls in parkinson's disease. *Brain*, 133(1):215–224, 2009.

[15] Lili Guo, Huan Xiong, et al. Dynamic rewiring of neural circuits in the motor cortex in mouse models of parkinson's disease. *Nature neuroscience*, 18(9):1299, 2015.

[16] URL `http://www.epda.eu.com/`.

[17] . URL `https://en.wikipedia.org/`.

[18] Fai Tsang and Tuck Wah Soong. Interactions between environmental and genetic factors in the pathophysiology of parkinson's disease. *IUBMB life*, 55(6):323–327, 2003.

[19] BAJ Veldman, AM Wijn, et al. Genetic and environmental risk factors in parkinsons disease. *Clinical neurology and neurosurgery*, 100(1):15–26, 1998.

[20] URL `http://parkinson.org/`.

[21] Shankar J Chinta, Georgia Woods, et al. Cellular senescence is induced by the environmental neurotoxin paraquat and contributes to neuropathology linked to parkinsons disease. *Cell reports*, 22(4):930, 2018.

[22] Erwin B Montgomery Jr. Heavy metals and the etiology of parkinson's disease and other movement disorders. *Toxicology*, 97(1-3):3–9, 1995.

[23] G Pezzoli, M Canesi, et al. Hydrocarbon exposure and parkinsons disease. *Neurology*, 55(5):667–673, 2000.

[24] GF Wooten, LJ Currie, et al. Are men at greater risk for parkinsons disease than women? *Journal of Neurology, Neurosurgery & Psychiatry*, 75(4):637–639, 2004.

[25] URL `http://www.parkinson.it/`.

[26] O Blin, AM Ferrandez, J Pailhous, and G Serratrice. Dopa-sensitive and dopa-resistant gait parameters in parkinson's disease. *Journal of the neurological sciences*, 103(1):51–54, 1991.

[27] Alice Nieuwboer, Gert Kwakkel, et al. Cueing training in the home improves gait-related mobility in parkinsons disease: the rescue trial. *Journal of Neurology, Neurosurgery & Psychiatry*, 78(2):134–140, 2007.

[28] Tamar C Rubinstein, Nir Giladi, et al. The power of cueing to circumvent dopamine deficits: a review of physical therapy treatment of gait disturbances in parkinson's disease. *Movement Disorders*, 17(6):1148–1160, 2002.

[29] Jacques Darcourt, Jan Booij, et al. Eanm procedure guidelines for brain neurotransmission spect using 123 i-labelled dopamine transporter ligands, version 2. *European journal of nuclear medicine and molecular imaging*, 37(2):443–450, 2010.

[30] David J Brooks. Imaging approaches to parkinson disease. *Journal of Nuclear Medicine*, 51(4):596–609, 2010.

[31] Raúl de la Fuente-Fernández. Role of datscan and clinical diagnosis in parkinson disease. *Neurology*, 78(10):696–701, 2012.

[32] Christopher G Goetz, Barbara Tilley, et al. Movement disorder society-sponsored revision of the unified parkinson's disease rating scale (mds-updrs): Scale presentation and clinimetric testing results. *Movement disorders*, 23(15):2129–2170, 2008.

[33] W Birkmayer, P Riederer, et al. The potentiation of the anti akinetic effect after l-dopa treatment by an inhibitor of mao-b, deprenil. *Journal of Neural Transmission*, 36(3-4):303–326, 1975.

[34] Galit Kleiner-Fisman, Jan Herzog, et al. Subthalamic nucleus deep brain stimulation: Summary and meta-analysis of outcomes. *Movement Disorders*, 21(S14), 2006.

[35] Letterio Morgante, Francesca Morgante, et al. How many parkinsonian patients are suitable candidates for deep brain stimulation of subthalamic nucleus? results of a questionnaire. *Parkinsonism & related disorders*, 13 (8):528–531, 2007.

[36] Carolina Pinto de Souza, Clement Hamani, et al. Spinal cord stimulation improves gait in patients with parkinson's disease previously treated with deep brain stimulation. *Movement Disorders*, 32(2):278–282, 2017.

[37] Andrea Landi, Andrea Trezza, et al. Spinal cord stimulation for the treatment of sensory symptoms in advanced parkinson's disease. *Neuromodulation: Technology at the Neural Interface*, 16(3):276–279, 2013.

[38] Ph L Gildenberg. Treatment of spasmodic torticollis with dorsal column stimulation. In *Advances in Stereotactic and Functional Neurosurgery 2*, pages 65–66. Springer, 1977.

[39] Nikolaus Wenger et al. Closed-loop neuromodulation of spinal sensorimotor circuits controls refined locomotion after complete spinal cord injury. *Science translational medicine*, 6(255):255ra133–255ra133, 2014.

[40] . URL `https://en.wikipedia.org/`.

[41] Paul Kaufmann, Kevin Englehart, and Marco Platzner. Fluctuating emg signals: Investigating long-term effects of pattern matching algorithms. In *Engineering in Medicine and Biology Society (EMBC), 2010 Annual International Conference of the IEEE*, pages 6357–6360. IEEE, 2010.

[42] Mohammadreza Asghari Oskoei and Huosheng Hu. Support vector machine-based classification scheme for myoelectric control applied to upper limb. *IEEE transactions on biomedical engineering*, 55(8):1956–1965, 2008.

[43] Jerome Friedman, Trevor Hastie, and Robert Tibshirani. *The elements of statistical learning*, volume 1. Springer series in statistics New York, 2001.

[44] Tomislav Milekovic, Tonio Ball, Andreas Schulze-Bonhage, Ad Aertsen, and Carsten Mehring. Detection of error related neuronal responses recorded by electrocorticography in humans during continuous movements. *PloS one*, 8(2):e55235, 2013.